THE JOURNAL OF BIOLOGICAL CHEMISTRY VOL. 283, NO. 25, pp. 17503–17514, June 20, 2008

Control of Excitatory Synaptic Transmission by C-terminal Src Kinase*[S]

Received for publication, February 4, 2008, and in revised form, April 28, 2008 Published, JBC Papers in Press, April 29, 2008, DOI 10.1074/jbc.M800917200

Jindong Xu[‡1], Manjula Weerapura[§1], Mohammad K. Ali[¶], Michael F. Jackson[§], Hongbin Li[§], Gang Lei[‡], Sheng Xue[‡], Chun L. Kwan[‡], Morris F. Manolson[‡], Kai Yang[§], John F. MacDonald[§2], and Xian-Min Yu[‡¶3]

From the [‡]Faculty of Dentistry, University of Toronto, Toronto, Ontario M5G 1G6, Canada, the [§]Department of Physiology, University of Toronto, Toronto, Ontario M5S 1A8, Canada, and the [¶]Department of Biomedical Sciences, College of Medicine, Florida State University, Tallahassee, Florida 32306-4300

The induction of long-term potentiation at CA3–CA1 synapses is caused by an *N*-methyl-D-aspartate (NMDA) receptor-dependent accumulation of intracellular Ca^{2+}, followed by Src family kinase activation and a positive feedback enhancement of NMDA receptors (NMDARs). Nevertheless, the amplitude of baseline transmission remains remarkably constant even though low frequency stimulation is also associated with an NMDAR-dependent influx of Ca^{2+} into dendritic spines. We show here that an interaction between C-terminal Src kinase (Csk) and NMDARs controls the Src-dependent regulation of NMDAR activity. Csk associates with the NMDAR signaling complex in the adult brain, inhibiting the Src-dependent potentiation of NMDARs in CA1 neurons and attenuating the Src-dependent induction of long-term potentiation. Csk associates directly with Src-phosphorylated NR2 subunits *in vitro*. An inhibitory antibody for Csk disrupts this physical association, potentiates NMDAR mediated excitatory postsynaptic currents, and induces long-term potentiation at CA3–CA1 synapses. Thus, Csk serves to maintain the constancy of baseline excitatory synaptic transmission by inhibiting Src kinase-dependent synaptic plasticity in the hippocampus.

Pyramidal neurons of the CA1 hippocampus receive excitatory synaptic input from the axons of CA3 pyramidal neurons, which form the Schaffer Collateral pathway. The induction of synaptic plasticity at these CA3–CA1 synapses requires stimulation of *N*-methyl-D-aspartate receptors (NMDARs)[4] located at CA1 pyramidal cell dendritic spine synapses. It is widely accepted that spine depolarization relieves the Mg^{2+} block of NMDARs, causing a concomitant increase in the influx of Ca^{2+}. Both long-term potentiation (LTP) and long-term depression (LTD) are triggered by the subsequent accumulation of intracellular Ca^{2+} in the spines. For example, induction of LTP increases Ca^{2+} up to 10 μM, whereas LTD is associated with lower but more sustained increases (1). Appreciable NMDAR-dependent Ca^{2+} influx occurs at spines even at resting membrane potential due to the relative incompleteness of the Mg^{2+} block (2). Therefore an NMDAR-dependent influx of Ca^{2+} occurs even at low, baseline frequencies of stimulation that induce neither LTP nor LTD. This raises a fundamental question: why does this baseline influx of Ca^{2+} fail to induce synaptic plasticity?

Part of the answer to this question may lie in the observations that the induction of LTP at these synapses also requires activation of the Src family tyrosine kinases, Fyn and Src (3). Src family kinases control the induction of LTP by potentiating the NMDAR-dependent influx of Ca^{2+} (3) and activation of Src is "necessary and sufficient" to induce LTP at CA3–CA1 neurons (4). Src facilitates NMDAR function likely by increasing tyrosine phosphorylation of the NR2A subunit, whereas Fyn does so by phosphorylating the NR2B subunit (3). The precise mechanism whereby Src and/or Fyn are activated during the induction of LTP is poorly understood. The influx of Ca^{2+} likely enhances the tyrosine kinase Pyk2, which associates with and activates Src (3, 5). Therefore, activation of NMDARs and an influx of Ca^{2+} are coupled to stimulation of Src, which is in turn responsible for increasing both NMDAR activity and the subsequent influx of Ca^{2+}. During high frequency stimulation, relief of the Mg^{2+} block of NMDARs is insufficient in itself for induction of long-term potentiation at CA3–CA1 synapses. This early Src-dependent positive feedback amplifies the NMDAR-dependent Ca^{2+} signal (6), allowing the activation of the appropriate downstream pathways (*e.g.* calcium/calmodulin-dependent kinase II) responsible for enhancing the surface expression (7) and/or function of AMPARs (8).

Surprisingly, during baseline stimulation intracellular applications of selective inhibitors of Pyk2 or Src are without effect on the amplitude of NMDAR-mediated excitatory postsynaptic currents (EPSCs) and thus fail to modify AMPAR-mediated EPSCs. However, they are highly effective in preventing the induction of LTP (4, 9). These results are not consistent with a

* This work was supported, in whole or in part, by National Institutes of Health Grant 5R01 NS053567-01 (to X. M. Y.). This work was also supported by grants from the Canadian Institutes of Health Research (to J. F. M.) and Ontario Heart and Stroke Foundation Grant NA5448 (to X. M. Y.). The costs of publication of this article were defrayed in part by the payment of page charges. This article must therefore be hereby marked "*advertisement*" in accordance with 18 U.S.C. Section 1734 solely to indicate this fact.

[S] The on-line version of this article (available at http://www.jbc.org) contains supplemental data and Figs. S1 and S2.

[1] Both authors contributed equally to this work.

[2] To whom correspondence may be addressed. Tel.: 416-978-2674; Fax: 416-978-4940; E-mail: j.macdonald@utoronto.ca.

[3] To whom correspondence may be addressed. Tel.: 850-645-2718; Fax: 850-644-5781; E-mail: xianmin.yu@med.fsu.edu.

[4] The abbreviations used are: NMDAR, *N*-methyl-D-aspartate receptor; PTPα, protein-tyrosine phosphatase α; LTP, long-term potentiation; LTD, long-term depression; AMPAR, alpha-amino-3-hydroxy-5-methyl-4-isoxazolepropionic acid; EPSC, excitatory postsynaptic current; EPSP, excitatory postsynaptic potential; GST, glutathione *S*-transferase; Ω, ohm; SH domain, Src homology domain; HEK, human embryonic kidney; Csk, C-terminal Src kinase; CT, C-terminal.

NMDAR-mediated Ca^{2+} entry into postsynaptic spines during the baseline stimulation (2). Indeed, such elemental Ca^{2+} signals might be expected to be amplified by Src-mediated facilitation of NMDARs (positive feedback), which would subsequently and progressively facilitate AMPAR-mediated EPSPs. Intuitively, such a scheme would be undesirable for the maintenance of a stable neuronal network. A regulatory mechanism may therefore exist that holds Src in balance while leaving NMDARs unaffected until they are required for the induction of synaptic plasticity (*e.g.* LTP).

Csk family kinases (Csk, COOH-terminal Src kinase and Chk, Csk-homologous kinase) are cytosolic kinases that inhibit Src family kinases and as such are possible candidates for such a regulatory mechanism. Reports showing the down-regulation of Csk in the adult brain and a parallel up-regulation of Chk suggest that Chk would be the most likely candidate (10, 11). However, we present evidence that Csk is present at CA3–CA1 synapses and that it interacts directly with the NMDAR complex to regulate the ability of Src to enhance NMDARs. Csk prevents an inappropriate activation of Src by the NMDAR-dependent influx of Ca^{2+} that occurs during baseline stimulation frequencies and, in turn, inhibits the induction of LTP. Ours is the first demonstration that Csk plays a critical role in regulating the balance between baseline synaptic excitatory transmission and plasticity in the adult central nervous system.

EXPERIMENTAL PROCEDURES

All animal experiments were conducted following the guidelines of the Canadian Council on Animal Care and the NIH, and were approved by the Animal Care Committee of the University of Toronto and the Animal Care and Use Committee of Florida State University.

Acutely Isolated CA1 Pyramidal Neurons and Electrophysiological Recordings—Methods for acute neuron isolation from young adult rats have been described previously (12). In brief, the hippocampi of postnatal (14–22 days) Wistar rats were dissected out and sliced into ~1-mm thick slices in ice-cold oxygenated extracellular solution and incubated for 45 min followed by digestion with 2–3 mg/ml crude papain extract for 30 min at room temperature. The slices were then washed and incubated at room temperature for an additional 1–2 h prior to use (see supplementary data).

Acutely isolated CA1 pyramidal neurons present both advantages and disadvantages as a preparation for examining the function of NMDAR-mediated currents. The isolation procedure shears off much of the dendritic tree leaving only a few major primary and secondary dendritic branches. Applications of NMDA during whole cell recordings will therefore induce currents mediated by the activation of channels largely found within the extrasynaptic compartment. Nevertheless, some synaptic NMDARs are likely stimulated as many synapses are located on the large dendritic processes that come along with the cell soma. The predominant subtype of NMDAR in the extrasynaptic compartment of CA1 pyramidal neurons is NR1/NR2B. However, it is estimated that ~25% of the receptor compliment in this compartment is composed of NR1/NR2A receptors. This contrasts with the ~75% compliment of this receptor subtype at the synapse (13). Furthermore, the peak open probability of NR1/2A receptors is about 2 to 5 times greater than for NR1/NRB receptors (14). It is therefore anticipated that populations of both NR1/NR2A and NR1/NR2B receptors will contribute substantially to the peak whole cell currents recorded from isolated CA1 pyramidal neurons. Of course, we cannot rule out the possible presence of triheteromeric receptors.

Whole cell-clamped pyramidal neurons are lifted into the stream of a rapid perfusion system (see below). One of the significant advantages to this preparation is the ability to rapidly apply agonists and antagonists to the entirety of each cell and to attain near equilibrium conditions that are similar to those used to study recombinant NMDAR currents expressed in HEK293 cells (15, 16). It is far more difficult, if not impossible, to achieve such conditions with cultured hippocampal neurons or with CA1 pyramidal neurons *in situ* in the slice preparation.

For whole cell recordings, acutely isolated neurons were bathed with the extracellular solution containing (mM): NaCl (140), KCl (5.4), 1.3 $CaCl_2$ (1.3), HEPES (25), glucose (33), tetrodotoxin (0.001), and glycine (0.003), pH 7.4, osmolarity 310–320 mOsm. Recording pipettes were filled with intracellular solution containing (mM): CsCl or CsF (140), HEPES (10), $MgCl_2$ (2), 1,2-bis(2-aminophenoxy)ethane-*N*,*N*,*N*′,*N*′-tetraacetic acid (1), and K_2ATP (4), pH 7.2, and osmolarity 290–300 mOsm. DC resistances of recording electrodes were 4–6 MΩ. Input resistance was monitored by applying a voltage step of −10 mV and any recordings with more than a 20% change during the recording were rejected. Only recordings with a pipette-membrane seal >2 GΩ were included.

For evoking NMDAR-mediated whole cell responses, the standard and NMDAR agonist-containing extracellular solutions were rapidly applied through double-barrel glass to neurons using the SF-77B fast-step perfusion system (Warner Instruments). Whole cell NMDAR-mediated currents were recorded using an Axopatch 1D or Axopatch 200B amplifier (Molecular Devices) under voltage-clamp and a holding potential of −60 mV except where otherwise indicated. For recordings from acutely isolated CA1 pyramidal neurons NMDA was applied at 50 μM in the continuing presence of 0.5 μM glycine. On-line data acquisition and off-line analysis were performed using pClamp8 software (Molecular Devices).

Hippocampal Slice Preparation and Electrophysiological Recording—Techniques used for the hippocampal slice preparation and electrophysiological recording have been previously described (9, 17). In brief, hippocampal slices (400 μm) were prepared from 3–4-week-old Wistar rats. Slices were recovered for 1 h in oxygenated artificial cerebral spinal fluid containing (mM): NaCl (124), KCl (3), $CaCl_2$ (2.6), $MgCl_2$ (1.3), $NaHCO_3$ (26), NaH_2PO_4 (1.25), and glucose (10), osmolarity 310–320 mOsm, pH 7.4. Recording electrodes were filled with an intracellular solution containing (mM): potassium gluconate (135.5), KCl (17.5), HEPES (10), EGTA (0.2), MgATP (2), GTP (0.3), and QX 314 (5) with osmolarity 290–300 mOsm, pH 7.2. DC resistances were 3–5 mΩ. Series resistance (10–30 megohms), monitored throughout the recording period, was estimated from the series resistance compensation of currents generated in response to 5-mV voltage steps. Cells were rejected if the resistance values changed by more than 20%. During recording, slices were continuously perfused at 3–5 ml/min

with oxygenated and heated (30–32 °C) artificial cerebral spinal fluid.

Synaptic responses were evoked with electrical stimulation at the border of the stratum radiatum-stratum lacunosum region. Stimuli were delivered at 0.05 or 0.1 Hz with the intensity adjusted to 25–30% of the maximal synaptic responses. Whole cell EPSCs or EPSPs were recorded from the CA1 cell body layer using Multiclamp 700A amplifier and Clampex 9 software (Molecular Devices). During whole cell recordings, field EPSPs (fEPSPs) were simultaneously recorded with electrodes filled with artificial cerebral spinal fluid and placed within the stratum radiatum. Whole cell EPSC recordings were conducted at −90 mV. After recording baseline synaptic activity for 10–30 min, tetanic stimulations (two 100 Hz stimulus trains; 500 ms with 10-s intertrain interval) were applied. The peak amplitudes of EPSCs and the slopes between 10 and 70% of the peak responses of EPSPs and fEPSPs were measured. Pharmacologically isolated NMDAR-mediated EPSPs were also recorded in some experiments with cells held at −60 mV in the presence of CNQX (10 μM) to block AMPARs and bicuculline to block $GABA_AR$ responses.

Biochemical Experiments-Subcellular Fractionation and PSD Isolation—Subcellular fractionation of adult male rat (40 to 60 days) forebrains were performed as previously described (18, 19, supplemental data). The approaches used for PSD isolation are described elsewhere (20–22). Briefly, the synaptosome fraction was isolated by discontinuous sucrose gradient centrifugation and solubilized in 0.5% Triton X-100, then centrifuged to obtain the PSD-I pellet. This pellet was re-suspended, solubilized in 0.5% Triton X-100, and centrifuged to obtain the PSD-II pellet. Extracts from individual fractions were finally solubilized in 1% SDS and centrifuged at 15,000 × *g* for 5 min for Western blot analysis.

Immunoprecipitation and Western Blot Analysis—Experiments were performed as described previously (9, 17). In brief, proteins from the P2 (or P1) fraction of adult rat forebrain were dissolved in a lysis buffer containing (mM): Tris-HCl (50, pH 9.0), NaCl (150), 0.5% (v/v) Triton X-100, 1% (w/v) sodium deoxycholate, 0.1% (w/v) SDS, EDTA (2), and sodium orthovanadate (1). For attached cell homogenates, cells were mechanically dissociated and cell pellets were re-suspended in HNTG buffer (50 mM HEPES, pH 7.5, 150 mM NaCl, 1% Triton X-100, 10% glycerol, 1 mM EDTA, 10 mM sodium pyrophosphate, 100 mM sodium fluoride, and 1 mM sodium orthovanadate). Solubilized proteins (600–800 μg) were incubated overnight at 4 °C with antibodies, as indicated. The immune complexes were collected with protein G-Sepharose beads (Amersham Biosciences) for 2 h at 4 °C. The blotting analysis was performed by repeated stripping and successive probing with antibodies as indicated. Antibodies used in these experiments include anti-NR1 (Pharmingen), NR2A C-terminal (Upstate), NR2A N-terminal (Santa Cruz), protein-tyrosine phosphatase α (PTPα) (17), Src (Oncogene), Src-Tyr(P)-416 (Cell Signaling), Src-Tyr(P)-527 (Cell Signaling), Chk (Santa Cruz), phosphotyrosine (Upstate), kv3.1b (BD Bioscience), and GluR2/3 (Upstate). Monoclonal ("anti-Csk," mouse, BD Biosciences) and polyclonal (rabbit, Santa Cruz) antibodies against Csk were used to avoid signal overlapping of Csk with IgG heavy chain in Western blotting. To avoid confusion, only the monoclonal Csk antibody raised against the SH2 and SH3 domains of Csk was labeled as anti-Csk in this paper. Non-selective mouse or rabbit IgG was utilized for immunoprecipitation as negative control.

cDNA Transfection—HEK293 or COS7 cells were transfected using the calcium phosphate method (Invitrogen) as per the manufacturer's instruction with expression vectors (pcDNA3 or pRcCMV) containing cDNAs encoding NR1-1a, full-length or C-terminal truncated NR2A, v-Src (a gift of Dr. T. Pawson, University of Toronto), Csk (a gift of Dr. K. Harder, Royal Melbourne Hospital), wild-type or mutant neuronal Src (n-Src, Y535F or K303R/Y535F, provided by Dr. S. Hanks, Vanderbilt University), and Src-(40–58) (a gift from Dr. M. W. Salter, Hospital For Sick Children, Toronto). To avoid confusion, the *n*-Src mutants of chicken c-Src used in our experiments are referred to as Y527F and K295R/Y527F. Transfected cells were maintained in Dulbecco's modified Eagle's medium with 10% fetal bovine serum for 24 h before lysis.

GST Pull-down Assay—pGEX2th-Csk-ST plasmid was kindly provided by Dr. G. Sun at the University of Rhode Island. Csk S109C mutation was made using QuikChange XL Site-directed Mutagenesis Kit (Stratagene) as described by the manufacturer. Point mutation was confirmed by DNA sequencing. The GST and GST fusion proteins conjugated with Csk or Csk S109C were produced in *Escherichia coli* (BL-21 strain, Invitrogen) with isopropyl β-D-thiogalactopyranoside (0.1 mM) induction. The bead-bound GST fusion proteins or GST alone (15–20 μg) were each incubated with solubilized membrane proteins (600–800 μg) extracted from the adult rat brain tissue or 5 μl of [^{35}S]methionine-labeled NR1 C-terminal (CT) peptide and NR2A CT peptide in binding buffer (2% bovine serum albumin in phosphate-buffered saline) overnight at 4 °C. Bound proteins were separated by electrophoresis and detected by Western blotting or autoradiography. [^{35}S]Methionine-labeled NR1 CT peptide and NR2A CT peptide were synthesized in the TnT T7 Quick Coupled Transcription/Translation System (Promega) following the protocol recommended by the manufacturer. For dephosphorylation treatment, 5 μl of [^{35}S]methionine-labeled NR2A CT peptide was incubated with 100 units of λ-protein phosphatase (New England Biolabs) in the reaction buffer prior to the pull-down assays (see supplemental data).

RESULTS

Due to the lack of highly selective inhibitors of Csk kinases we employed a Csk antibody (anti-Csk; mouse monoclonal antibody, 2.5 μg/ml, BD Biosciences) that prevents the ability of Csk to interact with NR2 subunits (see Fig. 7*B*) thereby inhibiting the ability of Csk to regulate the phosphorylation of NMDARs by Src. Such an approach is analogous to the use of anti-Src to selectively inhibit Src kinase activity in CA1 neurons (4). Intracellular applications of anti-Csk caused a time-dependent increase in the magnitude of the EPSP slope to 189 ± 11% of that recorded immediately after breakthrough (Fig. 1, *A* and *B*). The slope of the CA3–CA1 EPSP largely reflects the underlying AMPAR conductance when extracellular Mg^{2+} is present (*e.g.* 1.3 mM). The enhancement of EPSPs induced by the anti-Csk antibody application subse-

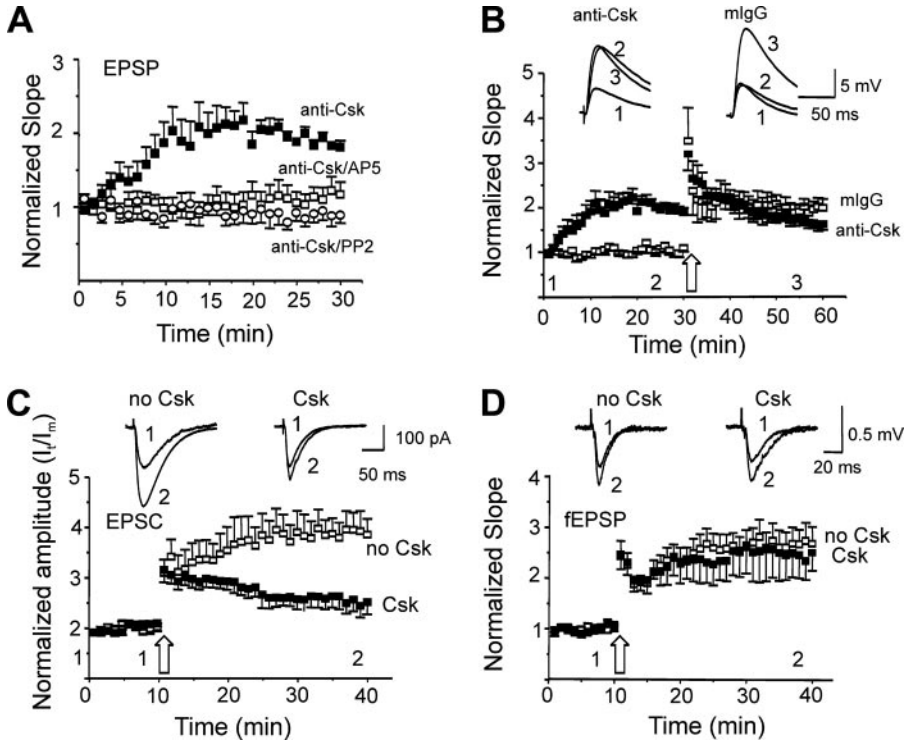

FIGURE 1. **Csk limits Src-dependent LTP at CA1 synapses.** *A,* the slopes of EPSPs were recorded from neurons during intracellular applications of anti-Csk (2.5 μg/ml, *closed squares*, $n = 6$) or during applications of the antibody in slices pre-treated with NMDAR antagonist AP5 (50 μM, *open squares*, $n = 7$) or SFK inhibitor PP2 (10 μM, *open circles*, $n = 5$). Slopes of EPSPs were normalized with respect to the values recorded at breakthrough. Anti-Csk substantially enhanced EPSP slopes during baseline stimulation ($p < 0.01$, Mann Whitney test). *B,* in two groups of cells anti-Csk (2.5 μg/ml, *closed squares*, $n = 6$) or non-selective mouse IgG (mIgG, 2.5 μg/ml, *open squares*, $n = 6$) was applied and subsequently LTP was induced. *C,* summary data (mean ± S.E.) showing the peak amplitudes of EPSCs (normalized with the mean values of EPSC peak amplitudes during the first 2 min: I_t/I_m) recorded from neurons during intracellular application of Csk (0.1 μg/ml, *closed squares*, $n = 6$) or no Csk (*open squares*, $n = 9$) and the attenuation of LTP ($p < 0.01$, Mann-Whitney test). *Insets* show examples of EPSCs recorded before (1) and after (2) the tetanus from neurons as indicated. *D,* slopes of fEPSPs normalized to the mean values of fEPSP slopes during the first 2 min. The fEPSPs were recorded simultaneously with the EPSC recordings shown in *C* with application of Csk (*closed squares*, $n = 6$) or no Csk (*open squares*, $n = 9$). *Insets* show examples of fEPSPs recorded before (*1*) and after (*2* and *3*) the tetanus. *Large open arrows* in *C* and *D* indicated tetanic stimulations. Time zero corresponds to the first evoked synaptic response (EPSP or EPSC as the case may be) recorded within 2 min after breakthrough, this brief delay being necessary to stabilize the recording.

quently occluded the induction of LTP (Fig. 1*B*). Furthermore, the potentiation of EPSPs by anti-Csk was blocked by pre-treating slices with the NMDAR antagonist AP5 (50 μM) or with the Src family kinase inhibitor PP2 (10 μM, 1 h) (Fig. 1*A*), indicating that endogenous Csk regulates synaptic plasticity through a Src family kinase and NMDAR-dependent mechanism.

We also examined the effects of recombinant Csk supplied through our patch pipette on EPSCs recorded in the whole cell voltage-clamp configuration. Intracellular applications of Csk had no time-dependent effect on the amplitude of baseline EPSCs (Fig. 1*C*), suggesting that endogenous Csk is sufficient to limit Src activity and prevent plasticity of baseline EPSCs. In contrast, recombinant Csk substantially attenuated the induction of LTP. In control recordings lacking Csk, the amplitude of EPSCs were significantly enhanced to 285 ± 32% (mean ± S.E., $n = 9$) after tetanic stimulation (Fig. 1*C*). However, application of recombinant Csk (0.1 μg/ml) into neurons through the recording pipettes substantially attenuated LTP of EPSCs (Fig. 1*C*). Recordings of fEPSPs performed simultaneously with whole cell recordings of EPSCs were used to confirm that the magnitude of LTP did not differ in slices from each treatment group (Fig. 1*D*).

We next considered if intracellular applications of Csk or its inhibitor (anti-Csk) would alter pharmacologically isolated NMDAR EPSCs. Csk caused no change in the amplitude of these NMDAR-mediated synaptic currents (Fig. 2*A*). In contrast, intracellular applications of anti-Csk caused a substantial and time-dependent increase in the amplitude of these currents that was not mimicked by a non-selective IgG (Fig. 2*B*). This anti-Csk induced enhancement was prevented by including the selective Src kinase inhibitory peptide (Src-(40–58)) in the patch pipette together with the antibody (Fig. 2*B*). These results imply that endogenous Csk kinases in CA1 neurons constitutively inhibit the Src-dependent potentiation of NMDAR EPSCs. Furthermore, this inhibition is likely complete, as supplementing the neurons with exogenous Csk kinase were without effect on these baseline responses.

To investigate the inhibitory effect of endogenous Csk on excitatory synaptic transmission, we first determined the subcellular distribution of Csk family kinases in the brain. Sequential fractionation of forebrain homogenates was performed from adult rats (40–60-days old). The NR1 subunit, PSD-95 (9, 18, 23), and Src (9, 18) were abundant in both the crude synaptosomal membrane (P2) and the synaptosomal membrane (LP1) fractions but little was detected in the synaptic vesicle-enriched (LP2), the low speed supernatant (S1, S2), or in the cytosolic (S3) fractions (Fig. 3*A*). In contrast, Csk and Chk were found in all the fractions but less Chk was apparent in the P2 and LP1 fractions where a strong NR1 signal was detected (Fig. 3*A*). Highly selective antibodies distinguishing between Csk and Chk were employed (supplemental Fig. S1).

Western blot analysis of the PSD fraction, which is highly enriched with the NR1 subunit and PSD-95, revealed that Src, Csk, and to a lesser degree Chk are also present in this fraction (Fig. 3*A*). The vesicle-associated membrane protein-2 was absent from this PSD fraction. Thus, we hypothesized that Csk family kinases and NMDARs may be closely associated in neurons.

To examine this hypothesis, we performed co-immunoprecipitation experiments using synaptosomal membrane preparations (P2 and LP1 fractions) solubilized under non-denaturing conditions. Both Csk kinases and NMDARs were located in

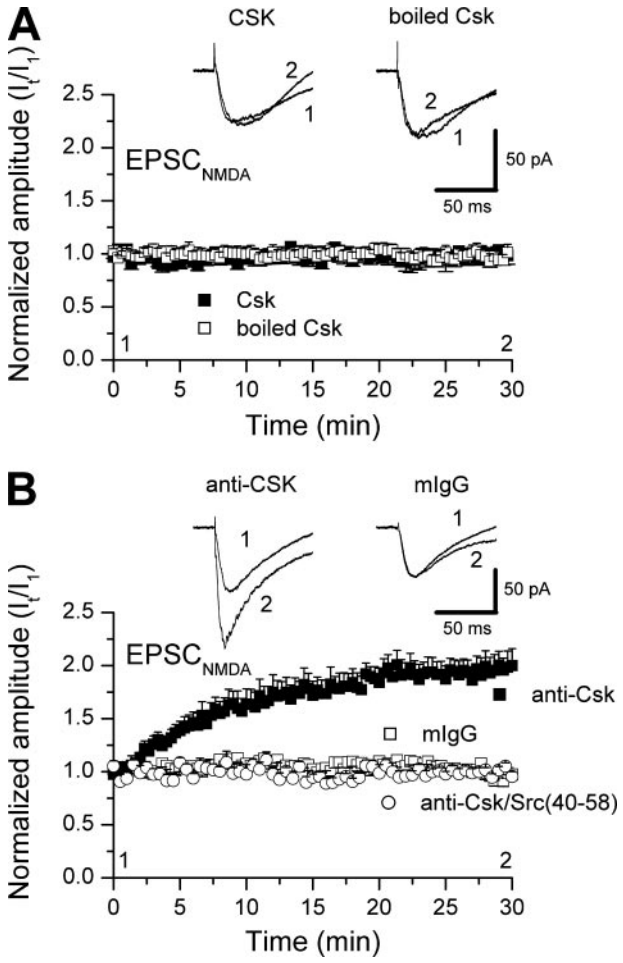

FIGURE 2. **Endogenous but not exogenous Csk down-regulates baseline NMDAR-mediated EPSCs in CA1 pyramidal neurons.** *A,* intracellular application of Csk (*closed squares*, $n = 7$) or boiled Csk (*open square*, $n = 5$) did not influence $EPSCs_{NMDA}$. *B,* intracellular application of anti-Csk (*closed squares*, $n = 6$) causes a progressive increase in the amplitude of pharmacologically isolated NMDAR-mediated EPSCs ($EPSCs_{NMDA}$) recorded in CA1 pyramidal neurons from hippocampal slices ($p < 0.01$, Mann Whitney test). Inclusion of a mouse non-selective IgG (mIgG, *open square*, $n = 6$) in the intracellular pipette solution was without effect. Co-application of the Src inhibitory peptide (Src-(40–58)) blocked the effects of anti-Csk on $EPSCs_{NMDA}$ (anti-Csk/Src-(40–58), *open circle*, $n = 6$). In both *A* and *B* the amplitude of $EPSCs_{NMDA}$ was normalized to their averaged amplitudes for the first minute after breakthrough: I_t/I_1. Representative traces in *A* and *B* were obtained at the times indicated by (*1*) and (*2*).

these fractions (Fig. 3*A*). An antibody against the NR1 subunit of the NMDAR precipitated neither Kv3.1b (24) nor GluR2/3 (23, 25) but did bring down NR2 subunits, PSD-95 (17, 25), Src (24, 25), and PTPα (17) (Fig. 3*B*). None of these proteins were detected in the immunoprecipitates obtained using a non-selective IgG (Fig. 3*B*). Importantly Csk, but not Chk, was found in NR1 immunoprecipitates (Fig. 3, *B* and *C*). Conversely, we also found that antibodies raised against Csk co-immunoprecipitated NMDAR subunits, PTPα and Src, but not Kv3.1b nor GluR2/3 (Fig. 3*D*).

In addition, NMDAR subunits, including NR1, NR2A, and NR2B, were pulled down from the brain using GST fusion proteins conjugated with Csk (GST-Csk), but not by GST alone (Fig. 3*E*). Neither Kv3.1b nor GluR2/3 was pulled down by GST-Csk and much less NMDAR protein was pulled down by Csk containing a defective SH2 domain (serine 109 mutated to a cysteine (GST-Csk S109C)) (26, 27) when compared with that using GST-Csk (Fig. 3*E*). These data indicate that Csk in the adult brain, but not Chk, complexes with NMDARs via its SH2 domain and forms a signaling complex together with PTPα and Src.

To further test the hypothesis that Csk regulates the abilities of Src to control NMDAR activity we turned to CA1 pyramidal neurons acutely isolated from hippocampal slices prepared from young adult rats. Recordings from these neurons are performed within 1 h of isolation and are therefore not to be confused with primary cultures of neurons. Concentrations of extracellular agonists and antagonists are tightly controlled using a rapid perfusion system.

Unlike the *in situ* slice condition, previous studies have shown that isolated CA1 neurons demonstrate enhanced Src kinase activity as NMDA-evoked currents are partially reduced by inhibitors of Src family kinases (4, 9). Extracellular application of the Src kinase inhibitor SU6656 (2 μM) inhibited NMDAR currents by about 40% (Fig. 4, *A* and *B*). Furthermore, including Csk (0.1 μg/ml) in the patch pipette led to a time-dependent depression of NMDAR currents to about 66% as compared with controls (Fig. 4, *C* and *D*). Csk did not alter the reversal potential or the decay time constant of NMDA currents (data not shown). In contrast, applications of boiled Csk had no effect on the amplitude of NMDA currents (Fig. 4*D*). We also confirmed the involvement of endogenous Src kinases by pre-treating neurons for 10 min with either of the Src family kinase inhibitors PP2 (10 μM) or SU6656 (2 μM) prior to breakthrough. Following this blockade of Src kinase Csk failed to inhibit NMDA currents (Fig. 4*D*). However, inhibition was spared when neurons were pretreated with the inactive analogue of PP2, PP3 (10 μM) (Fig. 4*D*). To determine whether Csk was specifically targeting Src as opposed to another Src family kinase such as Fyn, we also included the Src-selective inhibitor peptide Src-(40–58) in the patch pipette (3). The inhibition of NMDAR-mediated currents by Csk was also occluded by this inhibitor (Fig. 4*D*).

Given our results with isolated CA1 neurons we determined if there was any direct relationship between Csk and the Src-dependent phosphorylation of NR2A subunits expressed *in vitro* in HEK293 or COS7 cells. When both proteins were overexpressed in these cells, the NR2A subunit co-immunoprecipitated Csk (Fig. 5*A*). To examine the effects of increased tyrosine phosphorylation of NR2A on its association with Csk, we co-expressed Csk and NR2A along with v-Src. v-Src lacks the Csk targeting sequence in the C-tail (28) and was detected using an antibody that recognizes the autophosphorylated form of Src (Tyr-416) (Fig. 5*B*). Overexpression of v-Src did not alter the expression of NR2A or Csk but substantially enhanced the tyrosine phosphorylation of NR2A (Fig. 5, *A* and *B*). It also increased the amount of Csk that co-precipitated with NR2A (Fig. 5, *A* and *B*). The NR2A antibody failed to co-precipitate Csk in the absence of co-expressed NR2A (Fig. 5*A*) thus serving as a negative control. The greater the level of v-Src expression, the greater was both the phosphorylation of NR2A subunits and the co-precipitation of Csk (Fig. 5, *B*, *right panel,* and *D*). Overexpression of the constitutively active form of Src

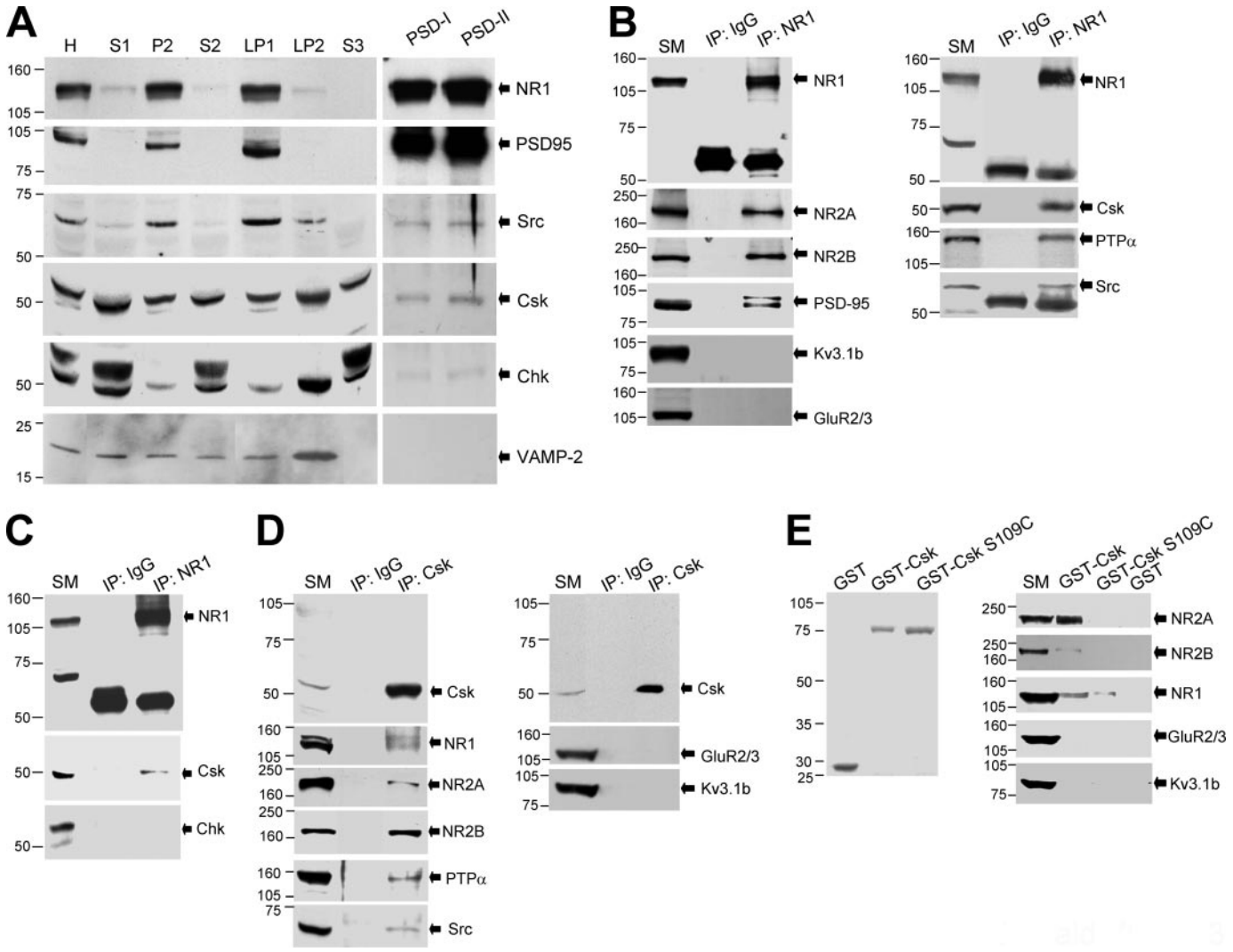

FIGURE 3. **Csk, PTPα, Src, and the NMDAR form a complex in the central nervous system.** *A*, subcellular fractionation profiles of the NMDAR NR1 subunit, PSD-95, Src, Csk family kinases, and vesicle-associated membrane protein-2 are illustrated. In each case 30 μg of protein was loaded into the lanes except the PSD lanes, where 5 μg was loaded. *B–D*, the gels were loaded with solubilized membrane protein (20 μg, *SM*) and immunoprecipitates (*IP*) of antibodies as indicated on the *top* of blots. *E*, *left panel* shows the Coomassie Blue staining of purified GST and GST fusion proteins after SDS-PAGE. The gel in the *right panel* was loaded with solubilized membrane proteins (120 μg, *SM*) and proteins were precipitated by GST fusion proteins as indicated on the *top* of blots. The filters were sequentially stripped and immunoblotted with antibodies against proteins as indicated next to the *arrows*. All experiments were repeated more than three times. *Numbers* to the *left* of blots indicate the position and size (kDa) of molecular mass markers. *H*, homogenate; *S1*, low-speed supernatant 1; *P2*, crude synaptosomal membrane; *S2*, low-speed supernatant 2; *LP1*, synaptosomal membrane; *LP2*, synaptic vesicle-enriched fraction; *S3*, cytosolic fraction; *PSD-I*, one Triton PSD pellet; *PSD-II*, two Triton PSD pellets.

(v-Src) also enhanced co-precipitation of NR2A together with endogenous Csk (supplemental Fig. S2*A*).

To determine whether this increase in Csk-NR2A co-precipitation was the result of an enhancement of Src kinase activity or, alternatively, if it was simply due to an increased expression of Src protein, we co-transfected cDNA encoding either constitutively active Src (C-tail Tyr-527 mutated to phenylalanine (Y527F)) or inactive Src (lysine 295) in kinase domain was mutated to arginine, in addition to the Tyr-527 mutation (Y527F/K295R) (29). The level of expression of Src was similar in these two groups of cells (Fig. 5*C*, *left panel)*, whereas the amount of Csk that co-precipitated with the NR2A subunit in cells expressing inactive Src was only 12 ± 3% ($n = 4$) of that in cells expressing active Src (Fig. 5, *C, right panel,* and *E*). Similarly, the co-expression of active Src also significantly enhanced the association of Csk with the NR2B subunit when compared with the co-expression of inactive Src (supplemental Fig. S2*B*). Csk was not precipitated with nonspecific IgG from the lysates of cells co-transfected with active Src (Fig. 5*C* and supplemental Fig. S2*B*). These findings demonstrate that association of Csk with NR2A (and NR2B) is dependent upon Src kinase activity.

Given the potential interactions between Csk and Src-induced phosphorylation of the NR2A subunit we explored the regions of NR2A that might directly interact with Csk. Wild-type or C-tail-truncated mutants of NR2A subunits were co-expressed in HEK293 cells together with NR1–1a, active Src (Y527F), and Csk (Fig. 6*A*). Csk was co-immunoprecipitated using antibodies directed against the N-terminal of NR2A subunits (Fig. 6*B*) or against NR1 subunits (Fig. 6*C*). Truncation of NR2A (amino acids 1–837) did not alter the assembly of NMDAR subunits (Fig. 6, *B* and *C*). However, it substantially

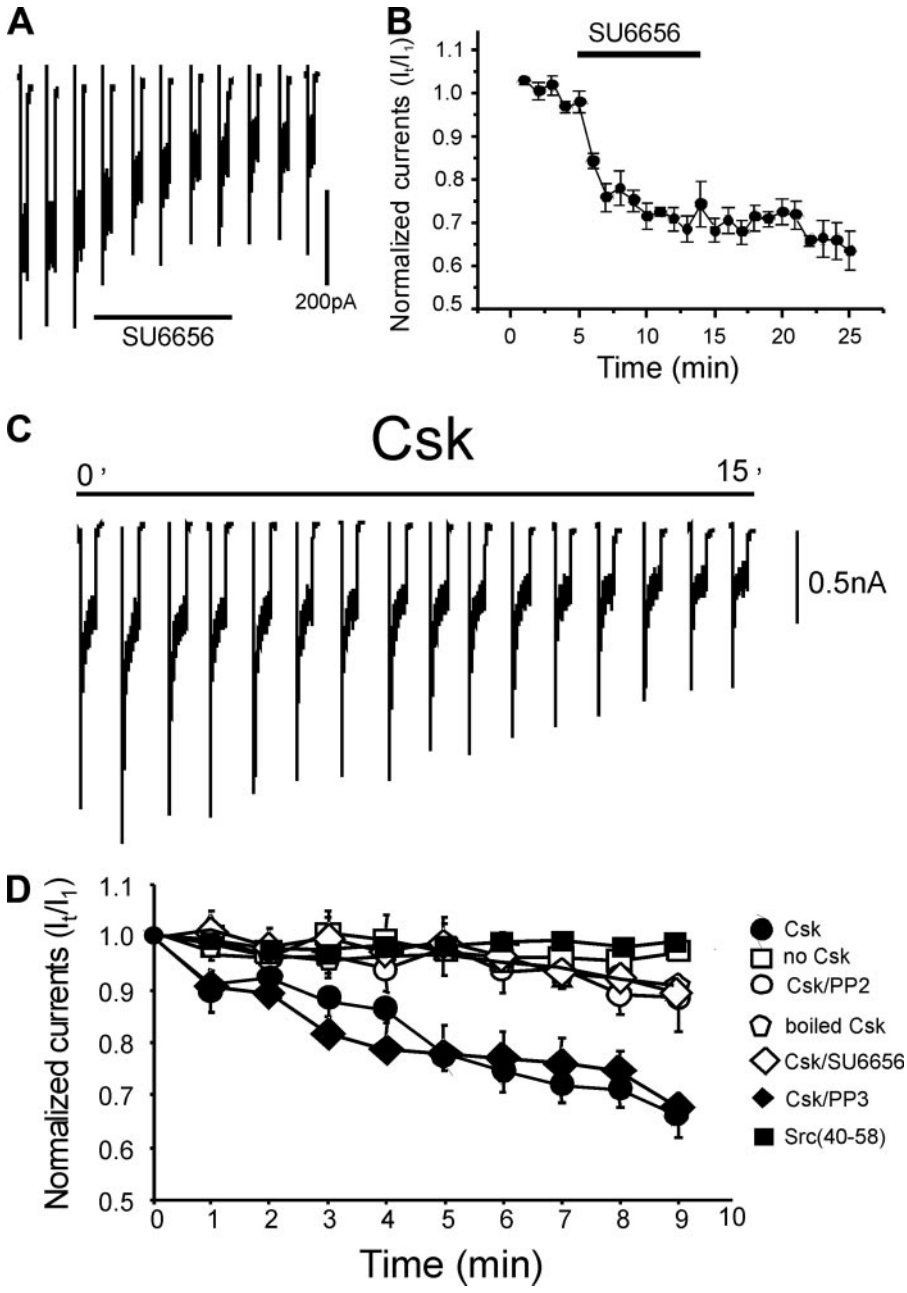

FIGURE 4. **Csk inhibits Src-dependent NMDAR-mediated whole cell currents in isolated hippocampal neurons.** *A*, acute inhibition of NMDA evoked currents during and following acute application of SU6656 (2 μM) at the time indicated by the *bar*. *B*, quantification of this inhibition for a series of cells ($n = 5$). *C*, example of NMDAR-mediated whole cell currents recorded from an acutely isolated CA1 neuron during intracellular application of Csk (0.1 μg/ml). Csk generated a time-dependent inhibition of these currents. *D*, summary data showing normalized amplitudes of NMDAR-mediated currents recorded in acutely isolated CA1 neurons from young rats. Seven groups of cells were compared: 1) those with no Csk (*open squares*, $n = 6$); 2) those with Csk (*closed circles*, $n = 7$); 3) those with Csk combined with the SFK inhibitor PP2 (10 μM) (*open circles*; $n = 5$); 4) those recorded with boiled Csk (*open hexagons*, $n = 5$); 5) those recorded with Csk and the SFK inhibitor SU6656 (2 μM) (*open diamonds*, $n = 8$); 6) those recorded with Csk and the inactive control PP3 (10 μM)(*closed diamonds*, $n = 5$); 7) those recorded with Csk and the Src-selective inhibitory peptide, Src-(40–58) (*closed squares*, $n = 6$). PP2, PP3, and SU6656 were added to the bath 10 min prior to recording NMDAR currents. Only Csk or Csk in the presence of PP3 demonstrated a time-dependent reduction in these currents ($p < 0.01$, Mann-Whitney test).

reduced co-immunoprecipitation of Csk (Fig. 6, *B–E*), confirming that Csk associates with the NMDAR complex through interactions involving the NR2A subunit C-terminal region.

We further characterized the interaction between Csk and NR2A by performing *in vitro* GST pull-down assays. Because increased tyrosine phosphorylation of NR2A increased its association with Csk we explored whether the SH2 domain of Csk is specifically responsible for binding to the NR2A subunit. SH2 domains serve as a binding site for phosphotyrosine residues (28, 30). The ^{35}S-labeled peptide corresponding to the C-tail (amino acids 838–1464) of the NR2A subunit was precipitated by GST-Csk but not by GST alone (Fig. 7*A*). When the experiment was repeated using GST fusion proteins conjugated with Csk containing a defective SH2 domain (26, 31) (GST-Csk S109C), much less NR2A C-tail peptide was pulled-down (Fig. 7, *A* and *B*). Furthermore, when the NR2A C-tail peptide was pretreated with λ-protein phosphatase (100 units, New England Biolabs), which reduced tyrosine phosphorylation of the NR2A C-tail peptide (Fig. 7*C*), the amount of NR2A C-tail peptide precipitated with GST-Csk was significantly reduced (Fig. 7, *A* and *B*).

Next, we examined the effects of the Csk antibody, anti-Csk (2.5 μg/ml), which was raised using a peptide sequence corresponding to the SH2-SH3 domains of Csk, on these interactions. Anti-Csk dose-dependently reduced the amount of NR2A C-tail peptide pulled down with GST-Csk (Fig. 7, *A* and *B*). However, it did not alter the *in vitro* kinase activity of Csk (data not shown). Applications of non-selective IgG produced no change in the pull-down of the NR2A C-tail peptide (Fig. 7, *A* and *B*). Therefore, Csk targets the tyrosine-phosphorylated NR2A subunit via its SH2 domain and application of anti-Csk prevents the interactions of Csk with the NR2A C-tail. By this means the antibody disrupts the interactions of Csk with NMDAR and thereby serves as a functional inhibitor of Csk action on NMDAR activity.

The activity of endogenous Src kinases, as well as the basal level of protein tyrosine phosphorylation of the NR2A subunit, is very low in HEK293 cells (Fig. 7, *D–G*) (32). Therefore, we examined the potential effect of Csk on tyrosine phosphorylation of the NR2A subunit in this cell line. Increasing Csk expression did not alter

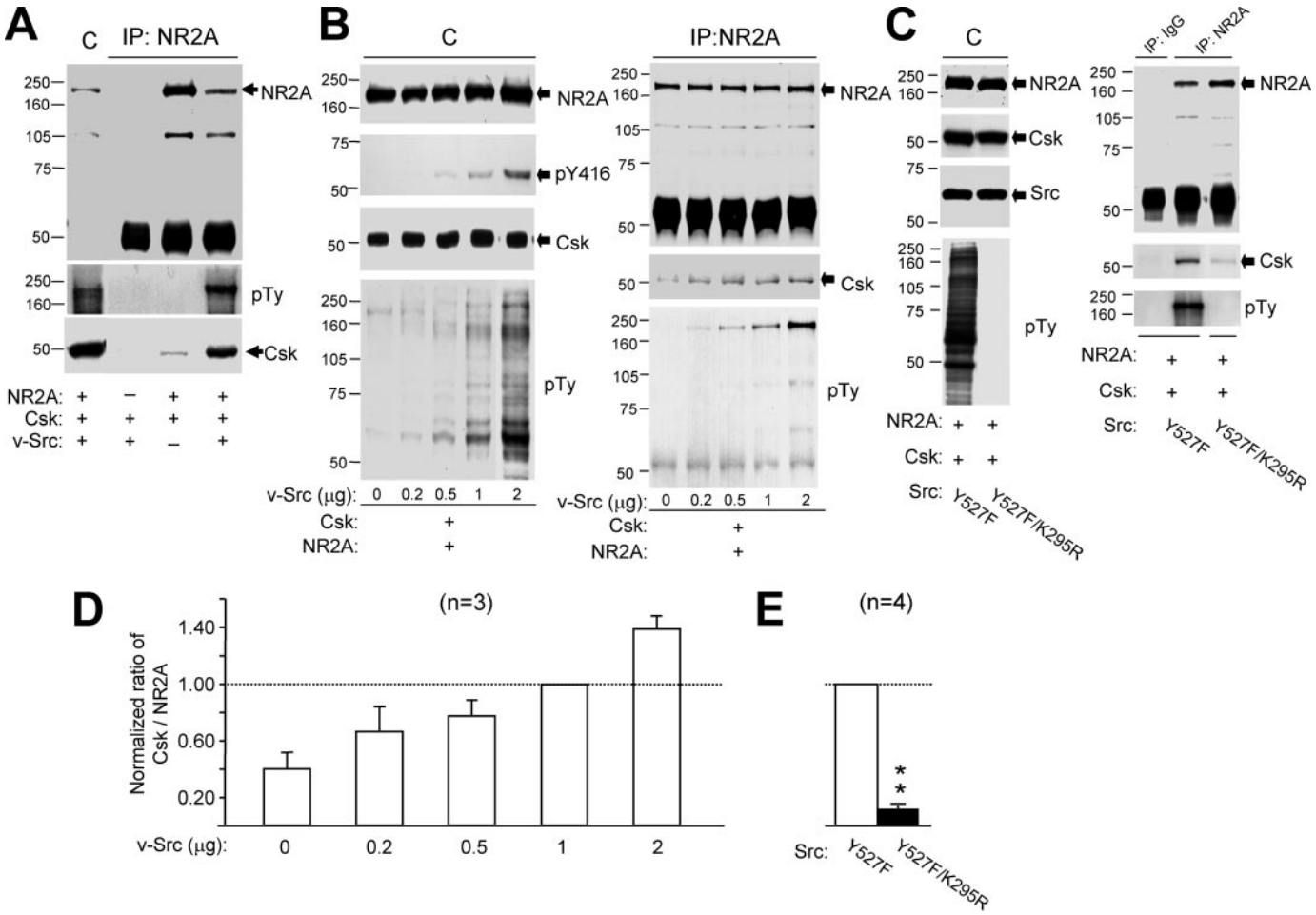

FIGURE 5. **Csk associates with the NR2A subunit by a Src-dependent mechanism.** *A,* gels were loaded (from left to right) with lysates (C) of HEK293 cells and immunoprecipitates of NR2A antibody from these cells transfected with and without cDNAs of proteins listed *below* the blot as indicated with "+" and "−," respectively. *B,* the gel (*left*) was loaded with lysates of cells co-transfected with various amounts of cDNAs encoding v-Src, and the gel to the *right* was loaded with NR2A immunoprecipitates from the lysates. *C,* the gel (*left*) was loaded with the lysates of cells co-transfected with cDNAs of active Src (Y527F) and inactive Src (Y527F/K295R), and the gels (*right*) were loaded with immunoprecipitates of non-selective IgG and NR2A antibody from the lysates. The filters were sequentially stripped and probed with antibodies against proteins as indicated to the *right* of blots. *D* and *E*, summary data (mean ± S.E.) showing the ratios of band intensities of Csk *versus* NR2A subunit protein detected in the NR2A immunoprecipitates. These were normalized with that found from cells co-transfected with 1 μg of v-Src (in *D*) or active Src (in *E*) cDNA (*dashed line*). The number of times the experiments were repeated is indicated in *parentheses*. **, $p < 0.01$, Student's *t* test in comparison between cells expressing the active and inactive Src. *pTy*, phosphotyrosine; *pY416*, tyrosine 416 phosphorylated Src.

tyrosine phosphorylation of the NR2A subunit (Fig. 7, *F* and *G*), demonstrating that Csk does not directly phosphorylate NMDARs. Transfection of wild-type Src into HEK293 cells substantially elevated both Src kinase activity and overall protein tyrosine phosphorylation (Fig. 7, *D* and *E*). Co-expression of Csk in these cells inhibited Src kinase activity (decreased Tyr-416 phosphorylation and increased Tyr-527 phosphorylation of Src) and reduced the overall protein tyrosine phosphorylation (Fig. 7, *D* and *E*). Expression of constitutively active Src (Y527F) further augmented Src kinase activity and protein tyrosine phosphorylation, but in this situation Csk did not alter either Src kinase activity or overall tyrosine phosphorylation (Fig. 7, *D* and *E*). This result is consistent with a lack of inhibition of constitutively active Src by Csk. Tyrosine phosphorylation of the NR2A subunit was also depressed when Csk was co-transfected in cells expressing wild-type Src but not in cells overexpressing constitutively active Src (Fig. 7, *F* and *G*). These results demonstrate that Csk modulates Src-induced NMDAR tyrosine phosphorylation of the NR2A subunit.

DISCUSSION

The importance of Src family kinases in the development of the central nervous system is well known but their specific role in synaptic transmission in the adult is less well recognized. Disruption of the *csk* gene in mice ($Csk^{-/-}$) leads to enhanced Src family kinase activity, resulting in severe defects in neural tube development and early (E9–10) embryonic lethality (27, 33) thereby illustrating that Csk is essential for central nervous system development. In contrast, *Chk* null mice are viable and demonstrate no histological central nervous system abnormalities (34). Nevertheless, a role for Csk in the adult central nervous system had all but been ruled out based on the dramatic down-regulation of Csk expression and parallel up-regulation of Chk that occurs with central nervous system maturation (10, 11, 35–37). Unexpectedly, our results show that it is Csk that is

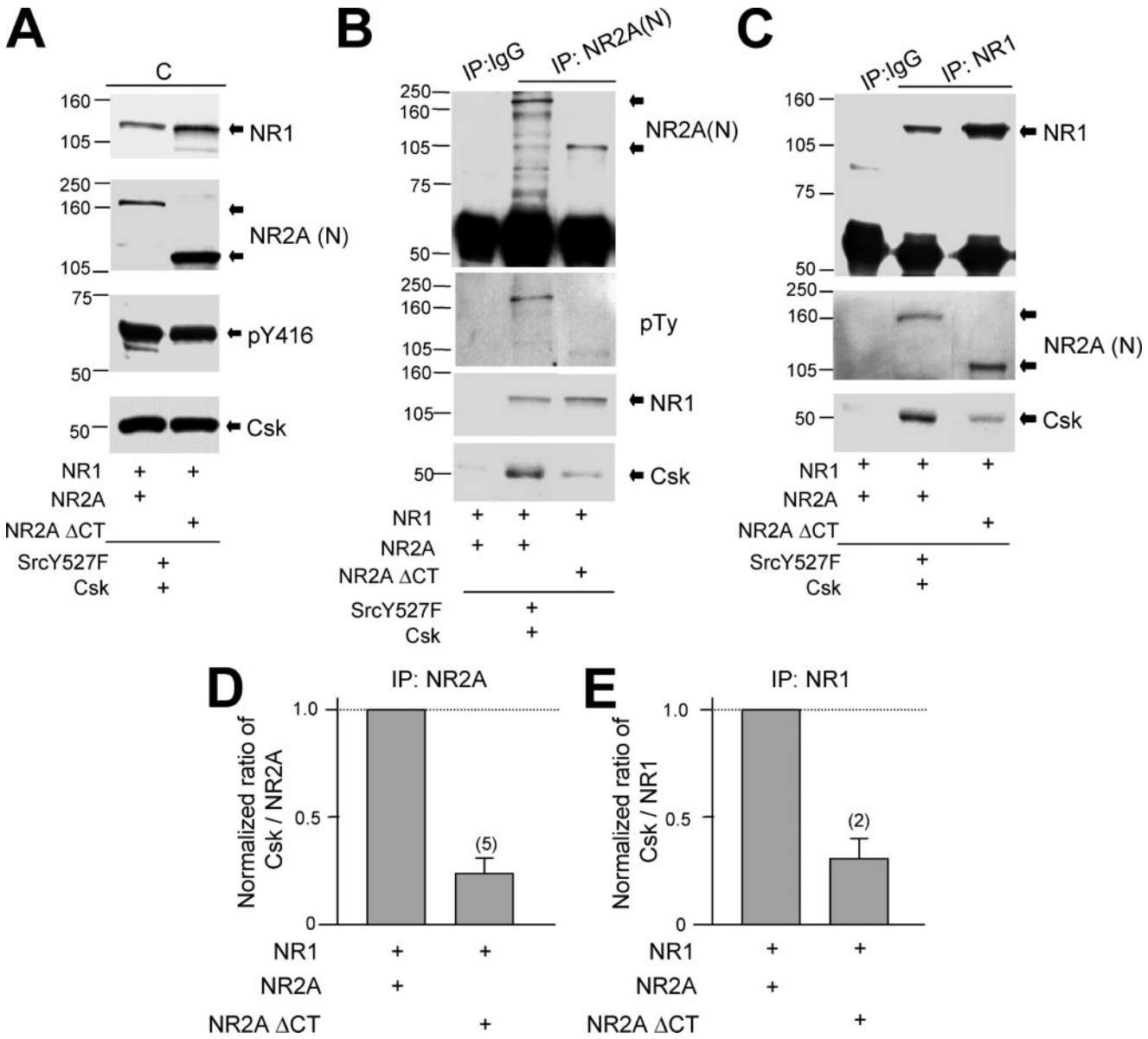

FIGURE 6. **NR2A subunit C-terminal is involved in Csk association with NMDARs.** *A,* gels were loaded with lysates of cells co-transfected with cDNAs of full-length NR1-1a and NR2A or C-tail truncated NR2A subunits as indicated. *B* and *C,* the gels were loaded with NR2A (IP:NR2A(N)) and NR1 (IP:NR1) immunoprecipitates from the lysates shown in *A*. The filters were sequentially stripped and probed with antibodies against proteins as indicated to the *right* of blots. *D* and *E,* summary data showing the ratios between the band intensities of Csk *versus* NR2A detected in the NR2A immunoprecipitates (*D*), and of Csk *versus* NR1 in the NR1 immunoprecipitates (*E*). These were normalized to those detected in cells expressing full-length NR1 and NR2A. The number of times the experiments were repeated is indicated in *parentheses*. NR2AΔ*CT*, C-tail truncated NR2A; *NR2A*(*N*), antibody against N-terminal of NR2A subunit.

a critical signaling molecule in controlling excitatory synaptic transmission and plasticity in the hippocampus.

In central neurons, Src increases the open probability of NMDA channels (24) and, in the absence of added extracellular Mg^{2+}, enhances NMDAR-mediated currents in cultured hippocampal, slice hippocampal, and acutely isolated CA1 neurons (4, 9, 17). This is likely achieved through phosphorylation of tyrosine residues on NR2A and NR2B subunits (3). For example, Src directly phosphorylates NR2A subunits and Fyn phosphorylates NR2B subunits (3). We have shown that application of recombinant Csk depresses NMDAR responses in acutely isolated CA1 pyramidal neurons taken from young rats. This depression was dependent upon Src family kinase activity as it was entirely occluded by pharmacological blockade using Src family kinase inhibitors (PP2, SU6656). It was also dependent upon the specific activation of Src kinase as it was blocked by the Src-selective inhibitory peptide, Src-(40–58) (3). Our results are consistent with Csk inhibiting Src and Fyn regulation of NR2A- and NR2B-containing receptors, respectively. Furthermore, we demonstrated that endogenous Csk depressed NMDAR-mediated EPSCs evoked by stimulation of Schaffer Collaterals.

We also provided evidence that Csk co-precipitates with the NMDAR complex of the adult brain along with Src and PTPα. To elucidate other potential physical associations, we examined the interaction of Csk with NMDAR subunits expressed in non-neuronal cells. We demonstrated co-immunoprecipitation of these proteins following overexpression of Csk and NR2A or

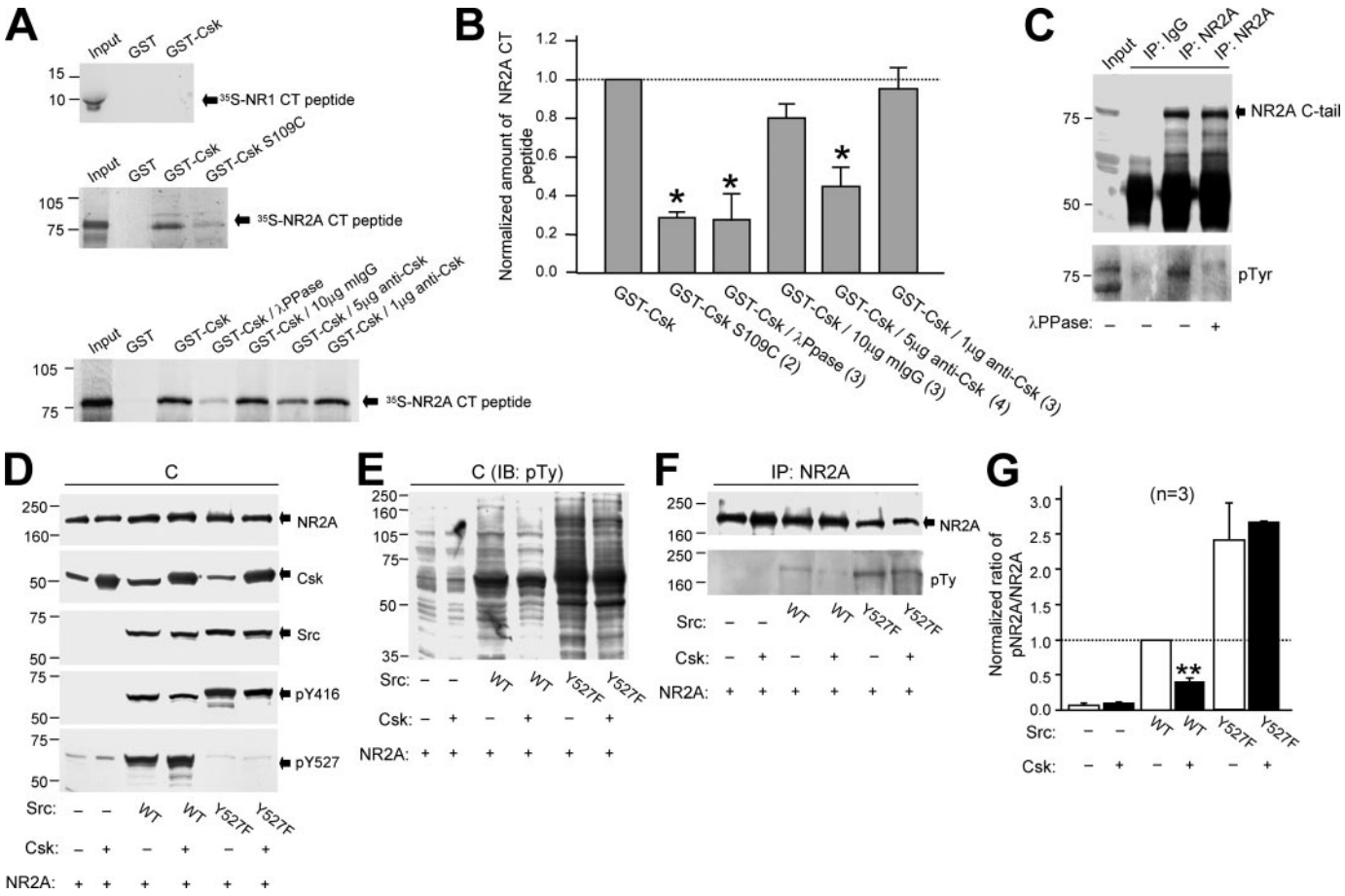

FIGURE 7. **Csk binds directly to the C-tail of the NR2A subunit *in vitro* and reduces NR2A subunit tyrosine phosphorylation in cells.** *A,* the *left panels* are autoradiographs showing ^{35}S-labeled peptide (*Input*, 10% of the total peptide used in the pull-down assays) corresponding to the C-tail of NR1 (^{35}S-NR1 CT peptide, *upper panel*) or NR2A subunit (^{35}S-NR2A CT peptide, *middle* and *lower panels*) pull-down by GST and GST fusion proteins conjugated with Csk (*GST-Csk*) or SH2 domain mutated Csk (*GST-Csk S109C*, *middle panel*). Peptides were synthesized with the TNT T7 Quick Coupled Transcription/Translation System (Promega). *B, bar graphs* showing the summarized data. *GST-Csk/λ-PPase*, GST-Csk-precipitated ^{35}S-NR2A CT peptide pre-treated with λ-protein phosphatase (100 units); *GST-Csk/10 μg non-selective IgG*, GST-Csk-precipitated ^{35}S-NR2A CT peptide in the presence of 10 μg of non-selective mouse IgG; *GST-Csk/5 μg anti-Csk*, GST-Csk-precipitated ^{35}S-NR2A CT peptide in the presence of 5 μg of anti-Csk; *GST-Csk/1 μg anti-Csk*, GST-Csk-precipitated ^{35}S-NR2A CT peptide in the presence of 1 μg of anti-Csk. *C,* the gel (from *left* to *right*) was loaded with NR2A C-tail peptide synthesized without isotope (*input*, 3% of total protein used in IP experiments), non-selective-IgG and NR2A immunoprecipitates (*IP*) from these TNT cell lysates with and without λ-protein phosphatase pre-treatment (1 h at 30 °C). *D* and *E*, the gels were loaded with lysates of cells transfected with cDNAs as indicated. *F*, the gel was loaded with NR2A immunoprecipitates from the cell lysates shown in *D* and *E*. *G*, summary data showing the ratios of band intensities of tyrosine-phosphorylated NR2A *versus* total NR2A detected in the NR2A immunoprecipitates. These were normalized to that detected in cells transfected with cDNAs encoding wild-type Src but without Csk overexpression (*dashed line*). Numbers in *parentheses* indicate the number of times the experiments were repeated. * and **, $p < 0.05$ and $p < 0.01$, Student's *t* test in comparison to the amount of NR2A CT peptide precipitated by GST-Csk without any treatment in *B*, and in comparison between wild-type Src expressing cells with and without Csk DNA co-transfection in *G*. *pY527*, tyrosine 527 phosphorylated Src; *WT*, wild-type; *Y527F*, active Src; *pTy*, phosphotyrosine; *IB*, immunoblotting.

NR2B subunits. Furthermore, as Src activity was increased and phosphorylation of NR2A and NR2B was enhanced, the association of Csk with the NR2A and NR2B subunits was also augmented. We conclude that the SH2 domain of Csk binds to NR2A and NR2B subunits in a tyrosine phosphorylation-dependent manner. This association likely brings Csk into proximity with Src and Fyn.

Increased Csk activity substantially attenuated NR2A subunit tyrosine phosphorylation in cells co-transfected with Src. In contrast, in cells expressing a mutant Src in which the C-tail tyrosine was mutated to phenylalanine, Csk activity failed to inhibit NR2A tyrosine phosphorylation. The endogenous level of Src family kinase activity and basal tyrosine phosphorylation of co-expressed NR2A subunits (32) is very low in HEK293 cells. This allowed us to examine the effect of increasing Csk activity under conditions of very low levels of basal Src activity. Overexpression of Csk failed to enhance tyrosine phosphorylation of NR2A subunits under these conditions indicating that Csk does not directly phosphorylate this subunit. Therefore, we conclude that Csk diminishes NMDAR tyrosine phosphorylation via the selective depression of Src kinase activity.

At CA3–CA1 synapses the induction of LTP requires the activation of Src family kinases Src and Fyn. The induction protocol itself activates these kinases, facilitates NMDAR activity, and in turn leads to the up-regulation of the synaptic AMPARs responsible for the enhanced EPSPs (38). However, inhibiting Pyk2, Src, or PTPα fails to alter the baseline AMPAR EPSPs recorded in CA1 pyramidal neurons even though they effectively prevent induction of LTP (4, 9, 17). This implies that Src activity, NMDARs, and the subsequent potentiation of EPSP amplitude is either subthreshold or that Src activity is

inhibited by endogenous Csk during baseline stimulation. Consistent with the later explanation, intracellular application of Csk did not alter baseline EPSPs in CA1 neurons but substantially reduced the Src-dependent induction of LTP at CA3–CA1 synapses. Basal Csk activity is apparently sufficient to keep Src in check because anti-Csk enhanced baseline currents and occluded subsequent induction of LTP. These results are also consistent with previous findings showing that intracellular applications of a Src-activator peptide lead to enhanced NMDAR and AMPAR currents and the occlusion of subsequent LTP (4), whereas Src inhibitors did not alter the strength of excitatory transmission themselves but did inhibit the induction of LTP (4).

Our results show that the association of Csk with the NMDAR complex is responsible for preventing the Src-dependent up-regulation of NMDARs, which would have occurred during baseline excitatory transmission at CA3–CA1 synapses. Csk also serves as an intrinsic mechanism to provide a "brake" on the induction of LTP by its phosphorylation of Src at its C-tail regulatory site. An additional brake to this induction is provided by striatal tyrosine-enriched phosphatase, which in contrast dephosphorylates tyrosine residues required for the activation of Src (39). On the other hand, PTPα dephosphorylates the regulatory C-tail tyrosine of Src family kinases and directly counteracts the inhibition of Src by Csk (17). Both Csk and PTPα therefore target phosphorylation of the C-tail tyrosine of Src kinases and provide a counterbalancing mechanism for the dynamic regulation of the induction of LTP at CA3–CA1 synapses.

Recent evidence indicates that Src family kinases serve as a convergent point of multiple transmitter pathways that in turn regulate NMDAR function in the hippocampus (3, 40–42). Postsynaptic receptors on CA1 neurons, which are capable of enhancing the activity of Csk, are anticipated to depress NMDAR activity contingent upon their up-regulation by Src family kinases. Csk is itself activated via a protein kinase A-dependent phosphorylation of serine 364 (43, 44). In this regard, the catalytic subunit of PKA depresses the up-regulation of single NMDA channel activity induced by the Src activator phosphopeptide EPQ(pY)-EEIPIA but fails to alter activity in the absence of this activator when applied to out-side out patches taken from cultured hippocampal neurons (45). This protein kinase A-dependent and Src-contingent inhibition of NMDAR currents is mimicked by stimulation of platelet-derived growth factor receptors (45), indicating a potential physiological mechanism whereby Csk regulates the level of baseline excitatory synaptic transmission in central neurons (42).

Csk interacts with NMDARs to inhibit their phosphorylation by Src. This Csk interaction is also dependent upon the degree of tyrosine phosphorylation of the NMDARs themselves. The greater the increase in phosphorylation of the receptor by Src, the greater will be the interaction with Csk. Therefore, Csk serves as a "governor" of the Src-dependent positive feedback of NMDARs that occurs during high frequency stimulation. By this means Csk not only regulates baseline CA1 transmission but also serves to limit the enhancement of NMDARs associated with LTP.

Acknowledgment—We thank Dr. M. W. Salter for reading and providing suggestions for this manuscript.

REFERENCES

1. Sobczyk, A., Scheuss, V., and Svoboda, K. (2005) *J. Neurosci.* **25,** 6037–6046
2. Bloodgood, B. L., and Sabatini, B. L. (2007) *Curr. Opin. Neurobiol.* **17,** 345–351
3. Salter, M. W., and Kalia, L. V. (2004) *Nat. Rev. Neurosci.* **5,** 317–328
4. Lu, Y. M., Roder, J. C., Davidow, J., and Salter, M. W. (1998) *Science* **279,** 1363–1367
5. Seabold, G. K., Burette, A., Lim, I. A., Weinberg, R. J., and Hell, J. W. (2003) *J. Biol. Chem.* **278,** 15040–15048
6. Dineley, K. T., Weeber, E. J., Atkins, C., Adams, J. P., Anderson, A. E., and Sweatt, J. D. (2001) *J. Neurochem.* **77,** 961–971
7. Groc, L., and Choquet, D. (2006) *Cell Tissue Res.* **326,** 423–438
8. Soderling, T. R., and Derkach, V. A. (2000) *Trends Neurosci.* **23,** 75–80
9. Huang, Y. Q., Lu, W. Y., Ali, D. W., Pelkey, K. A., Pitcher, G. M., Lu, Y. M., Aoto, H., Roder, J. C., Sasaki, T., Salter, M. W., and MacDonald, J. F. (2001) *Neuron* **29,** 485–496
10. Kuo, S. S., Armanini, M. P., Phillips, H. S., and Caras, I. W. (1997) *Eur. J. Neurosci.* **9,** 2383–2393
11. Kuo, S. S., Moran, P., Gripp, J., Armanini, M., Phillips, H. S., Goddard, A., and Caras, I. W. (1994) *J. Neurosci. Res.* **38,** 705–715
12. Lu, W. Y., Xiong, Z. G., Lei, S., Orser, B. A., Dudek, E., Browning, M. D., and MacDonald, J. F. (1999) *Nat. Neurosci.* **2,** 331–338
13. Groc, L., Heine, M., Cousins, S. L., Stephenson, F. A., Lounis, B., Cognet, L., and Choquet, D. (2006) *Proc. Natl. Acad. Sci. U. S. A.* **103,** 18769–18774
14. Chen, N., Luo, T., Wellington, C., Metzler, M., McCutcheon, K., Hayden, M. R., and Raymond, L. A. (1999) *J. Neurochem.* **72,** 1890–1898
15. Priestley, T., Laughton, P., Myers, J., Le Bourdellés, B., Kerby, J., and Whiting, P. J. (1995) *Mol. Pharmacol.* **48,** 841–848
16. Chen, N., Luo, T., and Raymond, L. A. (1999) *J. Neurosci.* **19,** 6844–6854
17. Lei, G., Xue, S., Chery, N., Liu, Q., Xu, J., Kwan, C. L., Fu, Y. P., Lu, Y. M., Liu, M., Harder, K. W., and Yu, X. M. (2002) *EMBO J.* **21,** 2977–2989
18. Kalia, L. V., and Salter, M. W. (2003) *Neuropharmacology* **45,** 720–728
19. Dunah, A. W., and Standaert, D. G. (2001) *J. Neurosci.* **21,** 5546–5558
20. Carlin, R. K., Grab, D. J., Cohen, R. S., and Siekevitz, P. (1980) *J. Cell Biol.* **86,** 831–845
21. Petralia, R. S., Sans, N., Wang, Y. X., and Wenthold, R. J. (2005) *Mol. Cell. Neurosci.* **29,** 436–452
22. Cho, K. O., Hunt, C. A., and Kennedy, M. B. (1992) *Neuron* **9,** 929–942
23. Sans, N., Prybylowski, K., Petralia, R. S., Chang, K., Wang, Y. X., Racca, C., Vicini, S., and Wenthold, R. J. (2003) *Nat. Cell Biol.* **5,** 520–530
24. Yu, X. M., Askalan, R., Keil, G. J., II, and Salter, M. W. (1997) *Science* **275,** 674–678
25. Husi, H., Ward, M. A., Choudhary, J. S., Blackstock, W. P., and Grant, S. G. (2000) *Nat. Neurosci.* **3,** 661–669
26. Neet, K., and Hunter, T. (1995) *Mol. Cell. Biol.* **15,** 4908–4920
27. Imamoto, A., and Soriano, P. (1993) *Cell* **73,** 1117–1124
28. Brown, M. T., and Cooper, J. A. (1996) *Biochim. Biophys. Acta* **1287,** 121–149
29. Polte, T. R., and Hanks, S. K. (1997) *J. Biol. Chem.* **272,** 5501–5509
30. Cooper, J. A., Gould, K. L., Cartwright, C. A., and Hunter, T. (1986) *Science* **231,** 1431–1434
31. Sabe, H., Hata, A., Okada, M., Nakagawa, H., and Hanafusa, H. (1994) *Proc. Natl. Acad. Sci. U. S. A.* **91,** 3984–3988
32. Kohr, G., Eckardt, S., Luddens, H., Monyer, H., and Seeburg, P. H. (1994) *Neuron* **12,** 1031–1040
33. Nada, S., Yagi, T., Takeda, H., Tokunaga, T., Nakagawa, H., Ikawa, Y., Okada, M., and Aizawa, S. (1993) *Cell* **73,** 1125–1135
34. Hamaguchi, I., Yamaguchi, N., Suda, J., Iwama, A., Hirao, A., Hashiyama, M., Aizawa, S., and Suda, T. (1996) *Biochem. Biophys. Res. Commun.* **224,** 172–179
35. Chong, Y. P., Chan, A. S., Chan, K. C., Williamson, N. A., Lerner, E. C.,

Smithgall, T. E., Bjorge, J. D., Fujita, D. J., Purcell, A. W., Scholz, G., Mulhern, T. D., and Cheng, H. C. (2006) *J. Biol. Chem.* **281,** 32988–32999
36. Chong, Y. P., Mulhern, T. D., and Cheng, H. C. (2005) *Growth Factors* **23,** 233–244
37. Chong, Y. P., Mulhern, T. D., Zhu, H. J., Fujita, D. J., Bjorge, J. D., Tantiongco, J. P., Sotirellis, N., Lio, D. S., Scholz, G., and Cheng, H. C. (2004) *J. Biol. Chem.* **279,** 20752–20766
38. Ali, D. W., and Salter, M. W. (2001) *Curr. Opin. Neurobiol.* **11,** 336–342
39. Pelkey, K. A., Askalan, R., Paul, S., Kalia, L. V., Nguyen, T. H., Pitcher, G. M., Salter, M. W., and Lombroso, P. J. (2002) *Neuron* **34,** 127–138
40. Gerber, U. (2002) *Neuropharmacology* **42,** 587–592
41. Kotecha, S. A., and MacDonald, J. F. (2003) *Int. Rev. Neurobiol.* **54,** 51–106
42. MacDonald, J. F., Jackson, M. F., and Beazely, M. A. (2007) *Biochim. Biophys. Acta* **1748,** 941–951
43. Abrahamsen, H., Vang, T., and Tasken, K. (2003) *J. Biol. Chem.* **278,** 17170–17177
44. Yaqub, S., Abrahamsen, H., Zimmerman, B., Kholod, N., Torgersen, K. M., Mustelin, T., Herberg, F. W., Tasken, K., and Vang, T. (2003) *Biochem. J.* **372,** 271–278
45. Lei, S., Lu, W. Y., Xiong, Z. G., Orser, B. A., Valenzuela, C. F., and MacDonald, J. F. (1999) *J. Biol. Chem.* **274,** 30617–30623